Spatio-temporal aspects of snowpack runoff formation during rain-on-snow

Sebastian Würzer[a] and Tobias Jonas[a]

[a]WSL Institute for Snow and Avalanche Research SLF
Flüelastrasse 11, 7260 Davos Dorf, Switzerland

Corresponding author:
Sebastian Würzer, sebastian.wuerzer@slf.ch, phone +49-1631639889

Key words:
runoff generation, mountain hydrology, rain-on-snow, snowmelt, spatiotemporal variability

This article has been accepted for publication and undergone full peer review but has not been through the copyediting, typesetting, pagination and proofreading process which may lead to differences between this version and the Version of Record. Please cite this article as doi: 10.1002/hyp.13240

Abstract

Rain-on-snow (ROS) is a complex phenomenon leading to repeated flooding in many regions with a seasonal snow cover. The potential to generate floods during ROS depends not only on the magnitude of rainfall, but also on the areal extent of the antecedent snow cover and the spatio-temporal interaction between meteorologic and snowpack properties. The complex interaction of these factors makes it difficult to accurately predict the effect of snow cover on runoff formation for an upcoming ROS event. In this study, the detailed physics-based snow cover model SNOWPACK was used to assess the influence of snow cover properties on converting rain input to available snowpack runoff during 191 ROS events for 58 catchments in the Swiss Alps. Conditions identified by the simulations that led to excessive snowpack runoff were a large snow covered fraction, spatially homogeneous snowpack properties, prolonged rainfall events and a strong rise in air temperature over the course of the event. These factors entail a higher probability of snowpack runoff occurring synchronously within the catchment, which in turn favors higher overall runoff rates. The findings suggest that during autumn and late spring, flooding due to ROS is more likely to happen, whereas during winter a coincidence of the above conditions in the study area is quite rare. For example, an autumn event which occurred in October 2011 resulted from a combination of spatially-homogeneous snowpack conditions following a recent snowfall and high, but not exceptional rainfall, and led to major flooding. The results of this study provide key factors to assess in advance of an incoming ROS event and emphasize the importance of detailed snow monitoring for flood forecasting in snow-affected watersheds.

1. Introduction

Many regions of the world experience rain on snow (ROS) situations on a regular basis. Il Jeong and Sushama (2017) report that 80 % of the annual January to May maximum daily runoff for large parts of Northern America is associated with ROS events. Additionally, for some parts of Austria, Merz and Blöschl (2003) determined 55 % of the annual peak flows to stem from ROS. While common, ROS situations do not necessarily lead to flooding. However, the biggest floods in those regions, involving severe damage and loss of lives, are often associated with ROS (e.g. Kroczynski, 2004; McCabe et al., 2007; Pomeroy et al., 2016; Wayand et al., 2015). The importance and unpredictability of those floods is reflected by the number of case studies dealing with their causative factors (e.g. Garvelmann et al., 2015; Kroczynski, 2004; Liu et al., 2016; Pomeroy et al., 2016; Rössler et al., 2014; Wever et al., 2014b).

Even though rainfall input usually dominates snow cover runoff for most ROS events, snowmelt can increase snow cover runoff by a factor of two during events with moderate rainfall totals, as compared to rainfall alone (Wayand et al., 2015; Würzer et al., 2016). The transient storage of rain water in the snowpack can conceptually be regarded as a part of the runoff routing processes of precipitation input to the catchment outlet (Blöschl, 2013) and therefore the snow cover can enhance or delay runoff formation processes and determine the timing of snowpack runoff (Lundquist et al., 2005). Resulting cumulative differences between snow cover runoff and rain input during a ROS event, henceforth referred to as runoff excess, is an important value when assessing a ROS event. It summarizes if the presence of a snow cover leads to additional runoff (positive runoff excess due to snowmelt) or if it retains water (negative runoff excess). While on the point scale complex snow cover processes and uncertainties in meteorological forecast make it difficult to accurately predict snowpack runoff, assessing ROS on the catchment scale additionally comprises to

deal with the spatial heterogeneity of snow cover properties and spatially variable meteorological inputs that influence both snowmelt and hydrological processes (Westrick & Mass, 2001). For example, high antecedent soil moisture is often observed during spring snowmelt conditions (Allan & Roulet, 1994; Fang & Pomeroy, 2016; Kampf et al., 2015; Webb et al., 2015; Wever et al., 2017) and can augment catchment runoff significantly. Preferential flow of liquid water through snow can have a distinct impact on timing and amount of snowpack runoff and has been examined using dye tracers (Schneebeli, 1995; Williams et al., 2010; Würzer et al., 2017), radar measurements (Albert et al., 1999), temperature investigations (Conway & Benedict, 1994), and by measuring the spatial variability of snowpack runoff (Kattelmann, 1989; Marsh, 1999; Marsh & Pomeroy, 1993; Marsh & Woo, 1985).

Frozen soils which coincide with the presence of snow and basal ice layers, often formed in prior ROS events (Würzer et al., 2017), can locally decrease the infiltration capacity of the soil. Under such circumstances, high snowpack runoff intensities can cause lateral overland flow, increasing the magnitude of runoff transported to the streams considerably (Bayard et al., 2005; Stähli et al., 2001; Teufel et al., 2017).

A delay of snowpack runoff after the start of rain may affect the runoff generation at the catchment scale, in particular if this time lag varies across the catchment. Further, air temperatures and snow cover extent usually do not support snowmelt in the whole catchment synchronously. Biggs and Whitaker (2012) found most snowmelt during spring to originate from critical elevation zones which only comprised a limited area of the catchment. White et al. (2002) found a strong relationship between the peak flow rate and the area contributing to melt depending on the catchment hypsometric curve. However, stream peakflow is higher when whole catchments generate runoff synchronously both for spring snowmelt (Lundquist et al., 2004) and during ROS (Garvelmann et al., 2015). Jones and Perkins (2010) concluded that prolonged precipitation and synchronized snowmelt from all areas of a catchment produce rapid and synchronized discharge responses and are the dominant controls on generation of extreme floods during ROS. Also Pomeroy et al. (2016)

mentioned the remarkable synchrony of flooding in all tributaries to the Bow River during Canada's most costly flood in June 2013. Whitfield and Pomeroy (2016) reported that particularly large flood events are the result of widespread ROS, suggesting that a large area affected by ROS probably has a bigger impact than high local snowmelt intensities. Physiographic controls like elevation influence depth, persistence, and properties of a snowpack and co-determine the location of the rain-snow-transition zone. For long lasting events which involve a substantial amount of snowmelt, higher elevations with persistent snowpacks become the primary source of catchment runoff (Garvelmann et al., 2015).

The basic requirements for ROS to happen are the presence of a snowpack and air temperatures that allow precipitation to fall as rain. With rising air temperatures, future climate will likely involve more precipitation falling as rain rather than snow. Therefore, ROS frequency, area, and runoff amount attributed to ROS is expected to rise in high-latitude (Il Jeong & Sushama, 2017; Putkonen & Roe, 2003; Ye et al., 2008) and mountainous regions (Il Jeong & Sushama, 2017; Köplin et al., 2014), where snow cover is still present during winter. However, ROS frequencies might decrease due to reduced snowfall and consequently less days with snow cover on the ground in mid-latitude regions or lower elevations (McCabe et al., 2007). Similar consideration also applies to a Swiss catchment, where increasing ROS frequencies are expected with rising air temperatures until further warming counteracts the initial effect (Beniston & Stoffel, 2016).

Large ROS-attributed floods have been studied with special regards to the coincidence in flood peak timing between small tributaries (Jones & Perkins, 2010), the spatial extent of ROS (Whitfield & Pomeroy, 2016) and the hydrological processes involved (Rössler et al., 2014). Yet there is little understanding of the role of snow cover properties and their spatial heterogeneity in supporting the synchronous generation of runoff within the catchment during ROS other than snow depth. These factors and the limited process representation in subsequent hydrological modeling (Rössler et al., 2014) make the runoff resulting from ROS events difficult to predict. Quite similar meteorological

conditions were shown to lead to significantly different consequences for different ROS events, dependent on antecedent snow cover conditions like liquid water content (LWC) (Kroczynski, 2004).

A ROS event which occurred in October 2011 in the Swiss Alps was - in terms of resulting damages - by far the biggest ROS event in the region for at least the last 15 years. Return periods for peak streamflow of 50-300 years were exceeding return periods for rainfall of several years by far (Badoux et al., 2013). This discrepancy in return periods was not expected by operational forecasters, which was partly attributed to a lack of experience with this type of ROS events and to insufficient process representation in the hydrological models used. To facilitate a better assessment of approaching ROS events, we have studied the influence of initial snow cover properties on converting rain input into snowpack runoff for as many as 191 ROS events within 58 catchments in the Swiss Alps. This paper addresses the following research questions:

- How do meteorology, initial snowpack properties, and topography jointly control runoff formation during ROS events? (RQ1)
- Are there particular combinations of storm, snowpack, and topography that entail an increased risk of excessive runoff and subsequent flooding? (RQ2)

To answer the above questions we used snow and meteorological data from a dense network of automatic weather stations in tandem with the physically based snow cover model SNOWPACK. Results from distributed snow cover simulations are first compared to corresponding results from point-scale simulations presented in Würzer et al. (2016) (Section 3.1). The spatial characteristics of snowmelt and rain retention zones for the investigated ROS events are presented in Section 3.2. The spatio-temporal course of the October 2011 ROS event is then presented in Section 3.3. RQ1 is addressed by identifying factors promoting synchronicity on the generation of runoff excess (Section 3.4), combinations entailing an increased risk of excessive runoff and subsequent flooding (RQ2) are discussed in Section 3.5.

2. Methods

All results in this study are derived from simulations with the one-dimensional physics-based snow cover model SNOWPACK, which is described in Section 2.3. The model was applied to virtual stations that were spatially distributed over 58 catchments in the Swiss Alps (See Section 2.2) to simulate a total of 191 ROS events. The virtual stations were generated to form a gridded representation of each catchment at 2 km horizontal spacing. The pre-processing library MeteoIO (Bavay & Egger, 2014) was used to extrapolate meteorological data from the IMIS (Interkantonales Mess- und Informationssystem) station network (Lehning et al., 1999), as described in Section 2.2. IMIS data have already been used for simulating ROS events with SNOWPACK in previous studies (Badoux et al., 2013; Wever et al., 2014b; Würzer et al., 2016).

2.1 Event Definition and Data Selection

The definition of a ROS event determines the number and spatio-temporal characteristics of events in a given record of meteorological data. To take the perspective of flood forecasting, our event definition is primarily based on precipitation in combination with an existing snow cover, as opposed to a runoff-based definition. However, we excluded spatially limited events which mostly occurred during summer months due to local convective precipitation events. The event selection was further limited to 15 winter (October to March) and 6 spring (April to May) events, where at least 5 of the IMIS stations experienced ROS at the same day. In the following, the term “event” refers to the above selection of 21 events which occurred simultaneously at multiple catchments. These events result in 191 individual records for a single catchment and event, hereafter referred to as a catchment event (CE). To classify as a CE, they had to fulfill the event definition used by Würzer et al. (2016): A ROS event is identified if a minimum of 20 mm of rainfall falls within 24 hours on a snowpack of at least 25 cm in depth at the onset of rainfall. The onset of an event was set to occur

when 3 mm of cumulative rain fell in the catchment. The end criterion was reached after less than 3 mm rain and runoff was simulated within 5 consecutive hours, respectively. Note that these definitions were adjusted from the original start and end criteria given in Würzer et al. (2016) as these were developed for a single location, not entire catchments as analyzed in this study.

2.2 Data

The boundaries of the catchments used in this study are defined according to the Swiss catchment classification scheme for, on average, domains of 150 km² (FOEN Federal Office for the Environment, 2015). Catchments were selected for this study if at least one IMIS station where a CE occurred was situated within its boundaries. This leads to a total of 58 catchments (Figure 1) ranging in size between 44 and 336 km².

The IMIS monitoring network was initially set up to serve the national avalanche forecast in Switzerland. It comprises automatic stations to measure both meteorological and snow parameters such as: wind speed and direction, air temperature, relative humidity, surface temperature, soil temperature, reflected shortwave radiation, and snow depth. Data is recorded at 30 minute intervals and further aggregated to arrive at a 1h model input dataset.

The following settings were used for MeteoIO to project available station data to the 2 km grid of virtual stations: The average environmental lapse rate (Daly et al., 2010) of -6.5 °C km^{-1} was considered for air temperature (TA). Relative humidity was distributed by the method described in Liston and Elder (2006). Wind speed measured at IMIS stations within the catchment (average wind speed, if more than one station) was uniformly distributed over the catchment. For incoming short wave radiation, a solar radiation interpolation scheme with terrain shading as described in Bavay and Egger (2014) was used. Incoming longwave radiative flux at each virtual station was simulated using the parameterization from Unsworth and Monteith (1975), coupled with a clear sky emissivity following Dilley and O'Brien (1998), as described in Schmucki et al. (2014). The rain gauges of IMIS

stations are unheated and therefore provide no reliable measurements in case of snowfall and mixed-phase precipitation, which is often observed during ROS. We therefore used a gridded 2 km precipitation dataset provided by MeteoSwiss (RhiresD, MeteoSwiss, 2013), as used in previous studies, to derive precipitation input for the SNOWPACK model (Würzer et al., 2016). The presence of canopy strongly affects the accumulation of snow and the energy balance and was found to significantly control snowmelt during ROS (Marks et al., 1998). A forest classification was derived from the Swiss land use statistics (FSO Federal Statistical Office, 2017), which separates 15 classes of land use. For the current study, we distinguished between three land use classes: forest, shrubland, and open. Forest canopy parameters used in the canopy module are described in Section 2.3.

2.3 Model Description & Setup

The physics-based snow cover model SNOWPACK represents the evolution of the snow cover in a 1-dimensional profile, which is comprised of a multitude of individual layers. A detailed description can be found in Bartelt and Lehning (2002), Lehning et al. (2002a), Lehning et al. (2002b), Lehning et al. (1999) and Wever et al. (2014a). The model is driven by hourly meteorological data as described in Section 2.2. Snowmelt occurs if the temperature of a layer exceeds 0°C and additional energy is provided. The energy input to the snow cover during melting conditions is calculated from radiative fluxes, turbulent heat fluxes, soil heat flux and advective energy provided by rain. The turbulent surface heat fluxes were simulated using a Monin–Obukhov bulk formulation for surface exchange (Lehning et al., 2002a). Stability correction functions of Stearns and Weidner (1993), as described in Michlmayr et al. (2008) were used to consider stable conditions. A dual domain approach based on the Richards' equation, which can account for the generation of preferential flowpaths, was chosen to model the transport of liquid water within the snowpack (Wever et al., 2016; Würzer et al., 2017). The model was initialized with a soil depth of 3 m to be able to accurately describe the heat and water flux between the soil and the snowpack. Soil heat flux at the lower boundary is set to a

constant value of 0.06 Wm^{-2} which is an approximation of the geothermal heat flux. In the absence of measured soil data, typical values for coarse soils were chosen to avoid ponding inside the snowpack due to saturated soil. A free drainage boundary condition was taken to prescribe the lower boundary condition for liquid water flow in the soil. In SNOWPACK, the canopy is represented by a 2-layer canopy module as described in Gouttevin et al. (2015), requiring information on canopy height, canopy closure and basal area. Canopy height is approximated to be 25 and 2 m for forest (evergreen conifers) and shrubland, respectively. Canopy closure (85 % for forest and 70 % for shrubland) and leaf area index (3 for forest and 2 for shrubland) was set according to Moeser et al. (2014). The basal area was set to be 40 $m^2\ ha^{-1}$.

3. Results and Discussion

3.1 Runoff formation at point versus catchment scale

Compared to runoff formation processes for an individual point or site, assessing processes for entire catchments additionally involves addressing the spatial dimension. We shall therefore contrast some considerations derived separately for these two scales. Similar to the approach chosen in this study, Würzer et al. (2016) simulated snow cover processes for ROS events using the SNOWPACK model and IMIS data, but only looked at locations of monitoring stations without considering between-station aspects. These simulations in combination with simulations presented in the current study enabled a direct comparison between results derived for both point locations and catchment areas (represented by the average value of all virtual stations from the equivalent simulation on a grid). Note that in this comparison there is typically one IMIS station (point scale) per watershed (catchment scale), see Figure 1.

Figure 2 shows the correlation between runoff excess and initial LWC for point simulations (Figure 2a) and catchment scale simulations (Figure 2b). For winter CEs which usually feature a rather low LWC, correlations are weak to non-existent for both scales. However, at the point scale there is a modest correlation between high initial LWC values and runoff excess (R^2=0.55), which is not the case for the catchment scale (R^2=0.16). This demonstrated that results derived for individual locations may not necessarily transfer into catchment-level findings. In this case, spatially heterogeneous snowpack properties add additional complexity to the problem and may dilute, cancel out, or even reverse effects that hold true for individual locations. Particularly, partial snow cover and asynchronous timing of runoff from different parts of a catchment does not typically allow as high runoff excess volumes as recorded for individual locations (Figure 2).

To further elaborate on this matter, we have tested a direct comparison of catchment and point scale runoff excess by associating results for individual IMIS stations with respective results for the catchments in which they reside. Figure 3 shows a rather weak correlation between both datasets (R^2 of 0.18 and 0.22 for winter and spring CEs, respectively). Generally, the range of runoff excess values is smaller when evaluated over catchments compared to individual locations. This may also lead to relatively few simulations showing an overall retention of runoff (negative excess) on the catchment scale, which is not the case for the point-scale simulations. This suggests that normally the area creating additional melt is larger than the area where rainwater is retained. In fact, only approximately 20 % of the CEs entail a retention area exceeding the area generating additional runoff excess. For events where both datasets show positive runoff excess, most of the catchment scale simulations result in runoff excess below the 1:1 line, which implies that often runoff excess at the IMIS station locations exceeds that calculated for the entire catchment. This is particularly the case for events in spring. Any part of the catchment that is not covered by snow attenuates the spatially averaged runoff excess. It is thus not surprising to find those paired simulations that reside above the 1:1 line to represent winter events exclusively, where snow free areas are typically sparse. The comparison also suggests that point scale simulations can obviously not be used as an

approximate upper limit for runoff excess values that are normally not exceeded at the catchment scale.

To further investigate the influence of the snow covered fraction (SCF) on runoff excess, we have included SCF in a multiple regression analysis of runoff excess at the catchment scale versus both runoff excess at the point scale and SCF. When we included SCF, the explained variance increased from 0.22 to 0.46, but only in the case of spring CEs. This suggests that SCF is a limiting factor for additional snowmelt during spring CEs. The above considerations are hampered by the fact that IMIS stations only represent a random location within each of the catchments considered here. We have therefore replaced the point simulations for the IMIS station locations with respective simulations for a point at the catchment's medium elevation and redone the regression analysis. With a R^2 of 0.47 for winter and 0.64 for spring CEs, the correlations were considerably improved, demonstrating that from a catchment hydrology perspective the placing of IMIS stations might not be optimal.

Highest and lowest values in Figure 3 are observed for point simulations, which suggests that an averaging behavior of processes is taking place on the catchment scale. This behavior can be attributed to spatially heterogeneous properties of the snow cover as well as storm properties resulting, e.g., from an elevational gradient. Zero-values for runoff excess from snow free areas and areas with snowfall are included in the mean runoff excess totals of the CEs.

The rather weak correlations for CE and point scale runoff excess show the limited applicability of point-scale observations for assessing ROS on the catchment scale. We therefore think it is necessary to analyze runoff generation behavior for ROS situations with a spatially distributed approach.

3.2 Snowmelt and retention zones during ROS

Before discussing the spatio-temporal course of the ROS events and the effects of meteorological and snowpack conditions on the catchment runoff generation, we shall first look at the elevational characteristics of the events investigated. Figure 4 (a) presents the mean cumulative runoff excess generation for each of the 21 events in 100 m elevation zones. The respective hypsometric curves are shown as profiles (in gray). Relative to the terrain, runoff excess (negative or positive) is only noted for a limited elevation range. Below the snowline, runoff excess is zero as rain input equals water available at the ground surface. Above the snowfall limit, there is no rain input and it is mostly too cold to melt so that consequently there is no runoff excess either. During autumn and winter events all simulations incorporate both areas that contribute additional runoff from snowmelt and areas that retain at least some rain water. Spring events, on the other hand, do not usually incorporate rainwater retention at any elevation. Areas leading to positive runoff excess are found generally at lower elevations for winter than for spring events, which is most apparent from Figure 4 (b). A similar seasonality in runoff excess has already been observed by Würzer et al. (2016).

Well-defined elevation zones which generate the majority of runoff excess can be regarded as the critical elevation zones during ROS. Similar to Biggs and Whitaker (2012), who analyzed runoff formation during spring snowmelt conditions, we identified such critical zones for the events analyzed here. Specifically we assessed which fraction of the catchment (represented by the fraction of grid cells) is at least needed to generate 75 % of the catchment runoff excess. This analysis revealed that in fact only 25 % and 40 % of the area was needed to generate 75 % of the runoff excess for winter and spring CEs, respectively. These percentages are equivalent of 300 and 500 m range in elevation. Rain water retention in at least some areas is one factor to explain why only a relatively small fraction of the catchment is involved in the generation of runoff excess in winter. During spring events, however, runoff excess is produced within a considerably larger fraction of the catchment area that is approximately equal to the SCF. This implies that the potential for snowmelt

is often exhausted during spring CEs. For the winter events, however, this is not the case and substantially more snowmelt could be generated if supported by current snowpack conditions and the energy balance. These findings illustrate that the potential for flood generation is indeed dependent on initial snowpack and meteorological conditions, since both factors determine the area that contributes snowmelt runoff. If we further include physiographic aspects, then snowmelt as well as runoff excess is normally restricted to a certain range in elevation. Whether or not this range coincides with a considerable portion of the catchment area is critically important for the effect of snow cover on runoff generation during ROS (Wayand et al., 2015).

3.3 Spatio-temporal course of a ROS event

During ROS, rain intensities, air temperatures, and snow cover conditions can change rapidly over the course of the event. Therefore, it is necessary to examine the spatio-temporal dynamics of the above factors. Figure 5 (a) shows the temporal course of runoff excess generation for a catchment during the October 2011 ROS event. Rain and snow cover runoff are displayed in Figure 5 (b) for the same observation period and catchment. In the beginning of the CE, rain was retained in the snow cover at nearly all elevations, leading to an overall negative runoff excess for the whole catchment. However, after some hours of intensive rain all elevations above the snowline started to contribute snowmelt, leading to an overall positive runoff excess for the whole catchment. In this case, synchronous timing of snowmelt between all snow-covered areas within the catchment not only increased the overall runoff, but also the maximum runoff intensity (by 20 % relative to the maximum rain intensity). Since high runoff intensities were found to produce fast overland flow (Bayard et al., 2005), synchronous timing of meltwater release over large fractions of the watershed may entail a greater risk of critical runoff rates and floods (Jones & Perkins, 2010).

3.4 Factors promoting the synchronized generation of runoff excess

A delay of snowpack runoff relative to the start of rain may affect the runoff behavior at the catchment scale, in particular if this time lag varies across a given catchment. Earlier studies have found short time lags being associated with high LWC and shallow snow covers (Würzer et al., 2016), suggesting that high catchment LWCs lead to spatially synchronous generation of runoff within the catchment. For our further spatial analysis, we define lag time as the time period between the onset of rain averaged across a given catchment (surpassing the 3mm threshold) and the onset of either runoff or rain at any individual location within the catchment. These rain and runoff lag times will typically vary in space. Figure 6 shows the standard deviation of runoff lag times as it relates to CE air temperatures, where colors denote the initial LWC. Here, the standard deviation of the runoff lag times is used as a proxy to measure synchronicity of the onset of runoff within a catchment, where low values denote high synchronicity and vice versa. The results show that this synchronicity is increasing with both air temperature and initial LWC. The data further imply that the effect of snow depth on lag time can only be of a limited nature if the initial LWC is high.

A multiple regression analysis was conducted to explain the variance in runoff synchronicity in terms of LWC, air temperature, and rain synchronicity. The above predictors explained 90 % of the variation in runoff synchronicity. While this is a good correlation, it is important to note that temperature and rain synchronicity are not independent from one another as temperatures determine the phase of precipitation. High enough temperatures therefore promote increased synchronicity in both rain input and snowmelt output.

At the point scale, snowpack runoff intensities were shown to be dependent on rain intensities as well as the event length (Würzer et al., 2016). Figure 7 shows a repetition of the analysis for the catchment scale (a) in comparison to the original results (b). The color differentiates between rain events lasting below and above 20 hours. For both spatial scales, snow cover processes attenuated rain intensities for most of the intense and short rain events (i.e. > 4 mmh^{-1} and < 20 h). Longer rain events, on the other hand, typically entailed an amplifying effect with only a few exceptions for the point scale and a fairly accurate match between rain and runoff intensities at the catchment scale. Also in this example catchment scale averaging processes seem to take place, which is why the ratio of runoff intensity to rain intensity is generally lower as compared to equivalent results from point scale simulations. In particular snow free areas equilibrate the overall ratio between rain and runoff as excess runoff is zero for these areas per definition.

Spatial compensating mechanisms between catchment processes mostly evolve due to the heterogeneous distribution of snow cover within the catchment. We therefore assessed the coefficient of variation (CV) of initial snow depth to characterize the heterogeneity. Respective CV values are shown against the maximum runoff excess intensity in Figure 8a, where colors denote the initial SCF. The data show that a low CV of initial snow depth is not necessarily indicative of high maximum runoff excess intensities, even though a tendency is present and high max. runoff excess intensities are only found for comparably low CV values. With increasing variability of snow cover, on the other hand, maximum catchment runoff intensities are considerably limited by the presence of a snow cover. For the SCF, the effect is the opposite: With a high SCF, a wide range of runoff excess intensities is possible, whereas low SCFs are necessarily associated with low maximum runoff excess intensities.

Figure 8b describes the relationship between mean runoff excess intensities and snow depth for point and catchment simulations (mean initial catchment snow depth). The highest runoff intensities are associated with shallow snow covers and deep snow covers are associated with low runoff intensities. Both datasets show a similar pattern, suggesting that high snow depths tend to moderate snowpack runoff intensities at both spatial scales. However, mean catchment values normally fall below values derived from point simulations, due to areas either retaining rain water or having snowfall instead of rainfall.

Results presented in Figure 8 support the assumption that a catchment which is widely covered by a homogeneous (Figure 8b) and shallow (Figure 8a) snow cover has the potential to generate high runoff excess intensities during ROS. Spatially variable snow cover characteristics and high initial snow depths, on the other hand, seem indicative of rather limited intensities of runoff excess.

3.5 Implications for forecasting runoff generation and flooding potential

Of all 21 events, the October 2011 event was by far the biggest of the analyzed events particularly in terms of the spatial extent (i.e. number of involved stations). The resulting damages and the inability of the operational forecast to predict the extreme nature of this particular event were motivation for several studies on ROS (Badoux et al., 2013; Rössler et al., 2014; Wever et al., 2014b). For this event, the return periods of rainfall were around several years, but resulting stream peak flows were in range of return periods of 50 to 300 years, which raised the question of which snow cover processes or other meteorological conditions led to extreme runoff rates (Badoux et al., 2013). Figure 9 may provide a clue; it displays the relationship between maximum runoff excess intensity and the change in air temperature over the duration of the event. Colors denote the increase in SCF over the 3 days before the start of rain and triangles mark CEs of the October 2011 event. The synopsis demonstrates that the October 2011 event was exceptional in combining a large increase of

SCF and a strong rise in air temperatures, which all together led to the highest runoff excess intensities of all 191 CEs. A recent snowfall down to low elevations in the days before the event led to large areas covered by fresh snow, providing a shallow homogeneous snow cover at a large SCF. We have seen above that these very conditions were both associated with high runoff intensities (Figure 8). A strong rise in air temperature over the course of the event further promoted a high synchronicity in the timing of runoff across the involved catchments (Figure 6).

In summary, the October 2011 event fulfilled four key criteria that have been identified in this study as indicative of high runoff excess and intensities (large SCF, shallow homogeneous snow cover, rising and high air temperatures; Figures 6, 8 and 9). In particular the above snow cover conditions seem most likely to occur in an autumn scenario, when a cold front results in the first significant snowfall for the season forming a shallow homogeneous snow cover over large parts of the catchment. Further into the winter season elevational snow distribution gradients usually build up, which prevent conditions similar to those recorded for the October 2011 event. Only towards the end of the snowmelt season a late snowfall down to low elevations might potentially entail comparable circumstances. But normally, SCF is a limiting factor in spring to prevent excessive runoff over extended areas.

As a contrasting example to the October 2011 event, the October 2000 event had less pronounced snow cover extent and the rain-snow transition zone during the event was lower due to declining air temperature over the course of the event. Consequently, rainfall and snowmelt were limited to lower elevations and relatively little catchment runoff excess for the CEs was reported. Nevertheless, because of extreme rainfall intensities at lower elevations, this event also led to localized floodings and debris flows, but, compared to the 2011 event, over a much reduced spatial extent. With higher air temperatures the consequences of this event could have been more devastating. The October 2011 event was limited by comparatively moderate rainfall amounts and the October 2000 event was limited by SCF and low air temperatures, yet despite these limitations, both events caused

considerable damages and economic losses, but still had the potential to generate even more runoff. It is therefore imperative to continuously monitor snow cover properties and other factors that allow for the accurate prediction of excessive runoff for a upcoming ROS event, to be able to prepare mitigation efforts where needed well in advance.

The multitude of interacting factors influencing synchronized and widespread snowmelt illustrate the challenge of accurately predicting runoff for an incoming ROS event. Many of these factors are difficult to assess, such as the spatial distribution of snowpack properties that are relevant but rarely measured anywhere (e.g. the LWC). Furthermore, there are always uncertainties in meteorological forecasts, which impact our ability to predict the amount, timing, and spatial distribution of precipitation and snowmelt (c.f. Rössler et al., 2014). The effect of snow cover on runoff excess and its synchronicity may be predicted most precisely for spring events: Since the snow cover usually has a high LWC and therefore its retention capacity is limited, short time lags and little retention can be expected. However, snowmelt during spring ROS is normally limited by the SCF. With high initial SCF, winter events usually exhibit a much higher potential for generating additional runoff. But these situations require a detailed knowledge of the spatial distribution of snowpack properties, its retention potential, and its thermal state, an assessment of which will remain challenging. Fortunately, as argued above, ROS events causing excessive runoff during winter seems the least likely scenario if compared to autumn and spring situations. However, warmer winter temperatures in future climate could increase the occurrence of mid-winter rain events.

Ultimately, the ability to predict the synchronicity in the timing of snowpack runoff for an incoming ROS event and a given catchment requires either an advanced snowmelt modeling system, or an assessment based on local expertise. The former may require the use of a physics-based snow cover model at a sufficient spatial resolution, adequate meteorological input data, and remote sensing information on SCF. The latter can likely benefit from studies like this one by identifying particular scenarios and precursors that potentially lead to high runoff excess and subsequent floods.

3.6 Results in the context of hydrological modelling

To improve the utility of studies like this, it would be desirable to further investigate the implications of ROS on the formation of fast runoff processes like lateral surface flow. Webb et al. (2017) stated that the spatial heterogeneity of soil moisture below the snowpack is less investigated than the state of the overlaying snow cover. Results from Kampf et al. (2015) show that longer snow persistence and wetter than average soil moisture conditions on a slope enable the development of saturation overland flow. Additionally, within the snowpack, certain processes remain difficult to assess. Würzer et al. (2017) and Juras et al. (2017) showed that preferential vertical flow of liquid water within a snowpack considerably influences rain water retention. Eiriksson et al. (2013) further revealed the importance of preferential lateral flow in sloped terrain for runoff formation in complex topography. In this study, we found that the snow cover processes considerably moderated the synchronicity of catchment runoff formation during ROS. However, any subsequent hydrological modeling critically depends on an accurate representation of runoff formation processes to be able to convert the water input at the soil surface to runoff at the catchment outlet in a realistic manner.

The results presented in this research strongly depend on the proper representation of snow cover processes by the model. This usually demands for a detailed validation of the model results. However, because of the sparse availability of spatially distributed measurements of LWC, snowmelt runoff and SWE - especially over large areas such as the catchments investigated in this study – such a direct validation of the model results seems unfortunately impossible. Yet the SNOWPACK model has been validated extensively in the past, including point scale simulations (Schmucki et al., 2014; Wever et al., 2014b), focussing on the water transport scheme within the model (Wever et al., 2014a; Wever et al., 2015; Würzer et al., 2017), and by distributed simulations using MeteoIO (Lehning et al., 2006; Schlögl et al., 2016; Wever et al., 2017). Schlögl et al. (2016) conducted a sensitivity analysis to systematically investigate the impact of different model setups on the robustness of modeled SWE and found that the input uncertainties of distributed simulations are in

the same range as uncertainties of SWE measurements. Most importantly, however, note that the snow model used in this study has been extensively validated using complementary snow depth, snow lysimeter, and snow pit data demonstrating its outstanding performance to simulate snowpack processes during ROS events in general, and to predict runoff lag times in particular (Würzer et al. 2017).

4. Conclusions

In this study we analyzed the effect of snow cover characteristics, meteorology and topography on converting rain input to snowpack runoff for 21 large-scale ROS events that occurred in 58 catchments in Switzerland between 2000 and 2011. The use of a physics-based snow cover model was particularly useful in assessing the role of the spatial variability of snow cover processes during ROS. The simulation results were used to identify controls and conditions that entailed increased runoff volumes and high runoff intensities.

Our analysis revealed that the following factors support extensive runoff:

A) spatially homogeneous snow cover conditions (Fig 8a)
B) shallow snow covers (Fig 8b)
C) high snow cover fraction (Fig 8a)
D) high / increasing air temperatures over the course of the ROS event (Fig 6 and Fig 9)
E) high initial LWC (Fig 6)
F) long lasting ROS events (Fig 7)

The above factors are all, directly or indirectly, connected to the likelihood of runoff being generated synchronously from the entire catchment, which in turn promotes high mean runoff intensities.

These findings show that ROS events leading to flooding in the study area are most likely to occur in autumn or towards the end of spring. A particular scenario could involve starting with a low SCF, then a cold front results in a snowfall forming a shallow homogeneous snow cover over large parts of the catchment, which is then followed by a considerable temperature rise and leads to extensive rain. Such a scenario automatically fulfills most of the above mentioned criteria. Under different meteorological conditions, ROS events are either limited by a low initial SCF in autumn and spring, or cannot support synchronous runoff generation due to pronounced spatial differences in snow cover properties in winter.

While the simulations complement meteorological and snow data for a large number of ROS events in Switzerland, the findings should apply to any region with similar meteorological and snow cover conditions.

Availability of data and model

Meteorological driving data for the SNOWPACK model (including all files required to set up and initialize the simulations) are available on the Envidat data portal at https://www.envidat.ch/dataset/ros_data. The SNOWPACK model is available under a LGPLv3 license at http://models.slf.ch. The version used in this study corresponds to revision 1249 of /branches/dev.

Acknowledgments

We thank the Swiss Federal Office for the Environment (FOEN) and the Laboratory of Cryospheric Sciences (CRYOS) at EPFL Lausanne, Switzerland for the funding of the project. Precipitation data (RhiresD and SwissMetNet) were provided by MeteoSwiss. We also would like to thank Janet Prevéy for proofreading of the manuscript.

References

Albert, M., Koh, G., & Perron, F. (1999). Radar investigations of melt pathways in a natural snowpack. *Hydrol. Process., 13*(18), 2991-3000. doi:10.1002/(SICI)1099-1085(19991230)13:18<2991::AID-HYP10>3.0.CO;2-5

Allan, C. J., & Roulet, N. T. (1994). Runoff generation in zero-order precambrian shield catchments: The stormflow response of a heterogeneous landscape. *Hydrol. Process., 8*(4), 369-388. doi:10.1002/hyp.3360080409

Badoux, A., Hofer, M., & Jonas, T. (2013). Hydrometeorologische Analyse des Hochwasserereignisses vom 10. Oktober 2011. . *Technical report, Birmensdorf, Swiss Federal Institute for Forest, Snow and Landscape Research WSL, in German, available at: http://www.wsl.ch/fe/gebirgshydrologie/wildbaeche/projekte/unwetter2011/Ereignisanalyse_Hochwasser_Oktober_2011.pdf (last access: 13 Sept 2017)*, 92pp.

Bartelt, P., & Lehning, M. (2002). A physical SNOWPACK model for the Swiss avalanche warning Part I: Numerical model. *Cold Reg. Sci. Technol., 35*(3), 123-145. doi:10.1016/S0165-232X(02)00074-5

Bavay, M., & Egger, T. (2014). MeteoIO 2.4.2: a preprocessing library for meteorological data. *Geosci. Model Dev., 7*(6), 3135-3151. doi:10.5194/gmd-7-3135-2014

Bayard, D., Stähli, M., Parriaux, A. l., & Flühler, H. (2005). The influence of seasonally frozen soil on the snowmelt runoff at two Alpine sites in Southern Switzerland. *J. Hydrol., 309*(1-4), 66-84. doi:10.1016/j.jhydrol.2004.11.012

Beniston, M., & Stoffel, M. (2016). Rain-on-snow events, floods and climate change in the Alps: Events may increase with warming up to 4°C and decrease thereafter. *Science of the Total Environment, 571*, 228-236. doi:10.1016/j.scitotenv.2016.07.146

Biggs, T. W., & Whitaker, T. M. (2012). Critical elevation zones of snowmelt during peak discharges in a mountain river basin. *J. Hydrol., 438-439*, 52-65. doi:10.1016/j.jhydrol.2012.02.048

Blöschl, G. (2013). *Runoff prediction in ungauged basins: synthesis across processes, places and scales*: Cambridge University Press.

Conway, H., & Benedict, R. (1994). Infiltration of water into snow. *Water Resour. Res., 30*(3), 641-649. doi:10.1029/93WR03247

Daly, C., Conklin, D. R., & Unsworth, M. H. (2010). Local atmospheric decoupling in complex topography alters climate change impacts. *International Journal of Climatology, 30*(12), 1857-1864. doi:10.1002/joc.2007

Dilley, A. C., & O'Brien, D. M. (1998). Estimating downward clear sky long-wave irradiance at the surface from screen temperature and precipitable water. *Quarterly Journal of the Royal Meteorological Society, 124*(549), 1391-1401. doi:10.1002/qj.49712454903

Eiriksson, D., Whitson, M., Luce, C. H., Marshall, H. P., Bradford, J., Benner, S. G., . . . McNamara, J. P. (2013). An evaluation of the hydrologic relevance of lateral flow in snow at hillslope and catchment scales. *Hydrol. Process., 27*(5), 640-654. doi:10.1002/hyp.9666

Fang, X., & Pomeroy, J. W. (2016). Impact of antecedent conditions on simulations of a flood in a mountain headwater basin. *Hydrol. Process., 30*(16), 2754-2772. doi:10.1002/hyp.10910

FOEN Federal Office for the Environment. (2015). Produktinformation Einzugsgebietsgliederung Schweiz (EZGG-CH). *Web document in German. (Available at https://www.bafu. admin. ch/dam/bafu/de/dokumente/wasser/fachinfo-daten/produktedokumentationeinzugsgebietsgliederungschweiz .pdf)*.

FSO Federal Statistical Office. (2017). Switzerland's Land Use Statistics (Arealstatistik der Schweiz, in German). *Web document in German. (Available at https://www.bfs.admin.ch/bfsstatic/dam/assets/6813/master)*.

Garvelmann, J., Pohl, S., & Weiler, M. (2015). Spatio-temporal controls of snowmelt and runoff generation during rain-on-snow events in a mid-latitude mountain catchment. *Hydrol. Process., 29*(17), 3649-3664. doi:10.1002/hyp.10460

Gouttevin, I., Lehning, M., Jonas, T., Gustafsson, D., & Mölder, M. (2015). A two-layer canopy model with thermal inertia for an improved snowpack energy balance below needleleaf forest (model SNOWPACK, version 3.2.1, revision 741). *Geoscientific Model Development, 8*(8), 2379-2398. doi:10.5194/gmd-8-2379-2015

Il Jeong, D., & Sushama, L. (2017). Rain-on-snow events over North America based on two Canadian regional climate models. *Climate Dynamics*, 1-14. doi:10.1007/s00382-017-3609-x

Jones, J. A., & Perkins, R. M. (2010). Extreme flood sensitivity to snow and forest harvest, western Cascades, Oregon, United States. *Water Resour. Res., 46*(12), W12512--. doi:10.1029/2009WR008632

Juras, R., Würzer, S., Pavlásek, J., Vitvar, T., & Jonas, T. (2017). Rainwater propagation through snowpack during rain-on-snow sprinkling experiments under different snow conditions. *Hydrol. Earth Syst. Sci., 21*(9), 4973-4987. doi:10.5194/hess-21-4973-2017

Kampf, S., Markus, J., Heath, J., & Moore, C. (2015). Snowmelt runoff and soil moisture dynamics on steep subalpine hillslopes. *Hydrol. Process., 29*(5), 712-723. doi:10.1002/hyp.10179

Kattelmann, R. (1989). Spatial Variability of Snow-Pack Outflow at a Site in Sierra Nevada, U.S.A. *Ann. Glaciol., 13*, 124-128. doi:10.3189/S0260305500007758

Köplin, N., Schädler, B., Viviroli, D., & Weingartner, R. (2014). Seasonality and magnitude of floods in Switzerland under future climate change. *Hydrol. Process., 28*(4), 2567-2578. doi:10.1002/hyp.9757

Kroczynski, S. (2004). A comparison of two rain-on-snow events and the subsequent hydrologic responses in three small river basins in Central Pennsylvania. *Eastern Region Technical Attachment, 4*, 1-21.

Lehning, M., Bartelt, P., Brown, B., & Fierz, C. (2002a). A physical SNOWPACK model for the Swiss avalanche warning Part III: Meteorological forcing, thin layer formation and evaluation. *Cold Reg. Sci. Technol., 35*(3), 169-184. doi:10.1016/S0165-232X(02)00072-1

Lehning, M., Bartelt, P., Brown, B., Fierz, C., & Satyawali, P. (2002b). A physical SNOWPACK model for the Swiss avalanche warning Part II: Snow microstructure. *Cold Reg. Sci. Technol., 35*(3), 147-167. doi:10.1016/S0165-232X(02)00073-3

Lehning, M., Bartelt, P., Brown, B., Russi, T., Stöckli, U., & Zimmerli, M. (1999). SNOWPACK calculations for avalanche warning based upon a new network of weather and snow stations. *Cold Reg. Sci. Technol., 30*(1-3), 145-157. doi:10.1016/S0165-232X(99)00022-1

Lehning, M., Völksch, I., Gustafsson, D., Nguyen, T. A., Stähli, M., & Zappa, M. (2006). ALPINE3D: a detailed model of mountain surface processes and its application to snow hydrology. *Hydrol. Process., 20*(10), 2111-2128. doi:10.1002/hyp.6204

Liston, G. E., & Elder, K. (2006). A Meteorological Distribution System for High-Resolution Terrestrial Modeling (MicroMet). *J. Hydrometeorol., 7*(2), 217-234. doi:10.1175/JHM486.1

Liu, A. Q., Mooney, C., Szeto, K., Thériault, J. M., Kochtubajda, B., Stewart, R. E., . . . Pomeroy, J. (2016). The June 2013 Alberta Catastrophic Flooding Event: Part 1: Climatological aspects and hydrometeorological features. *Hydrol. Process., 30*(26), 4899-4916. doi:10.1002/hyp.10906

Lundquist, J. D., Cayan, D. R., & Dettinger, M. D. (2004). Spring Onset in the Sierra Nevada: When Is Snowmelt Independent of Elevation? *J. Hydrometeorol., 5*(2), 327-342. doi:10.1175/1525-7541(2004)005<0327:SOITSN>2.0.CO;2

Lundquist, J. D., Dettinger, M. D., & Cayan, D. R. (2005). Snow-fed streamflow timing at different basin scales: Case study of the Tuolumne River above Hetch Hetchy, Yosemite, California. *Water Resour. Res., 41*(7). doi:10.1029/2004WR003933

Marks, D., Kimball, J., Tingey, D., & Link, T. (1998). The sensitivity of snowmelt processes to climate conditions and forest cover during rain-on-snow: a case study of the 1996 Pacific Northwest flood. *Hydrol. Process., 12*(10-11), 1569-1587. doi:10.1002/(SICI)1099-1085(199808/09)12:10/11<1569::AID-HYP682>3.0.CO;2-L

Marsh, P. (1999). Snowcover formation and melt: recent advances and future prospects. *Hydrol. Process., 13*(14-15), 2117-2134. doi:10.1002/(SICI)1099-1085(199910)13:14/15<2117::AID-HYP869>3.0.CO;2-9

Marsh, P., & Pomeroy, J. W. (1993). *The impact of heterogeneous flow paths on snowmelt runoff chemistry. In Proc. East. Snow. Conf., volume 61, pages 231-238*.

Marsh, P., & Woo, M. K. (1985). Meltwater Movement in Natural Heterogeneous Snow Covers. *Water Resour. Res., 21*(11), 1710-1716. doi:10.1029/WR021i011p01710

McCabe, G. J., Clark, M. P., & Hay, L. E. (2007). Rain-on-Snow Events in the Western United States. *Bulletin of the American Meteorological Society, 88*(3), 319-328. doi:10.1175/BAMS-88-3-319

Merz, R., & Blöschl, G. (2003). A process typology of regional floods. *Water Resour. Res., 39*(12). doi:10.1029/2002WR001952

MeteoSwiss. (2013). Documentation of MeteoSwiss Grid-Data Products, Daily Precipitation (final analysis): RhiresD. Technical report, Federal Office of Meteorology and Climatology MeteoSwiss, Zürich, Switzerland.

Michlmayr, G., Lehning, M., Koboltschnig, G., Holzmann, H., Zappa, M., Mott, R., & Schöner, W. (2008). Application of the Alpine3D model for glacier mass balance and glacier runoff studies at Goldbergkees, Austria. *Hydrol. Process., 22*(19), 3941-3949. doi:10.1002/hyp.7102

Moeser, D., Roubinek, J., Schleppi, P., Morsdorf, F., & Jonas, T. (2014). Canopy closure, LAI and radiation transfer from airborne LiDAR synthetic images. *Agricultural and Forest Meteorology, 197*, 158-168. doi:10.1016/j.agrformet.2014.06.008

Pomeroy, J. W., Fang, X., & Marks, D. G. (2016). The cold rain-on-snow event of June 2013 in the Canadian Rockies - characteristics and diagnosis. *Hydrol. Process., 30*(17), 2899-2914. doi:10.1002/hyp.10905

Putkonen, J., & Roe, G. (2003). Rain-on-snow events impact soil temperatures and affect ungulate survival. *Geophys. Res. Lett., 30*(4). doi:10.1029/2002GL016326

Rössler, O., Froidevaux, P., Börst, U., Rickli, R., Martius, O., & Weingartner, R. (2014). Retrospective analysis of a nonforecasted rain-on-snow flood in the Alps - a matter of model limitations or unpredictable nature? *Hydrol. Earth Syst. Sci., 18*(6), 2265-2285. doi:10.5194/hess-18-2265-2014

Schlögl, S., Marty, C., Bavay, M., & Lehning, M. (2016). Sensitivity of Alpine3D modeled snow cover to modifications in DEM resolution, station coverage and meteorological input quantities. *Environmental Modelling & Software, 83*, 387-396. doi:https://doi.org/10.1016/j.envsoft.2016.02.017

Schmucki, E., Marty, C., Fierz, C., & Lehning, M. (2014). Evaluation of modelled snow depth and snow water equivalent at three contrasting sites in Switzerland using SNOWPACK simulations

driven by different meteorological data input. *Cold Reg. Sci. Technol., 99*(0), 27-37. doi:10.1016/j.coldregions.2013.12.004

Schneebeli, M. (1995). *Development and stability of preferential flow paths in a layered snowpack. In Tonnessen, K., Williams, M., and Tranter, M., editors, Biochemistry of Seasonally Snow-Covered Catchments (Proceedings of a Boulder Symposium July 1995), pages 89-95, AHS Publ. no. 228.*

Stähli, M., Nyberg, L., Mellander, P.-E., Jansson, P.-E., & Bishop, K. H. (2001). Soil frost effects on soil water and runoff dynamics along a boreal transect: 2. Simulations. *Hydrol. Process., 15*(6), 927-941. doi:10.1002/hyp.232

Stearns, C. R., & Weidner, G. A. (1993). Sensible and Latent Heat Flux Estimates in Antarctica. In D. H. Bromwich & C. R. Stearns (Eds.), *Antarctic Meteorology and Climatology: Studies Based on AutomaticWeather Stations, Antarctic Research Series* (pp. 109-138): American Geophysical Union.

Teufel, B., Diro, G. T., Whan, K., Milrad, S. M., Jeong, D. I., Ganji, A., . . . Sushama, L. (2017). Investigation of the 2013 Alberta flood from weather and climate perspectives. *Climate Dynamics, 48*(9), 2881-2899. doi:10.1007/s00382-016-3239-8

Unsworth, M. H., & Monteith, J. L. (1975). Long-wave radiation at the ground I. Angular distribution of incoming radiation. *Q. J. Roy. Meteor. Soc., 101*(427), 13-24. doi:10.1002/qj.49710142703

Wayand, N. E., Lundquist, J. D., & Clark, M. P. (2015). Modeling the influence of hypsometry, vegetation, and storm energy on snowmelt contributions to basins during rain-on-snow floods. *Water Resour. Res., 51*(10), 8551-8569. doi:10.1002/2014WR016576

Webb, R. W., Fassnacht, S. R., & Gooseff, M. N. (2015). Wetting and Drying Variability of the Shallow Subsurface Beneath a Snowpack in California's Southern Sierra Nevada. *Vadose Zone Journal, 14*(8). doi:10.2136/vzj2014.12.0182

Webb, R. W., Fassnacht, S. R., & Gooseff, M. N. (2017). Hydrologic Flowpath Development Varies by Aspect during Spring Snowmelt in Complex Subalpine Terrain. *The Cryosphere Discussions, 2017*, 1-24. doi:10.5194/tc-2017-12

Westrick, K. J., & Mass, C. F. (2001). An Evaluation of a High-Resolution Hydrometeorological Modeling System for Prediction of a Cool-Season Flood Event in a Coastal Mountainous Watershed. *J. Hydrometeorol., 2*(2), 161-180. doi:10.1175/1525-7541(2001)002<0161:AEOAHR>2.0.CO;2

Wever, N., Comola, F., Bavay, M., & Lehning, M. (2017). Simulating the influence of snow surface processes on soil moisture dynamics and streamflow generation in an alpine catchment. *Hydrology and Earth System Sciences, 21*(8), 4053-4071. doi:10.5194/hess-21-4053-2017

Wever, N., Fierz, C., Mitterer, C., Hirashima, H., & Lehning, M. (2014a). Solving Richards Equation for snow improves snowpack meltwater runoff estimations in detailed multi-layer snowpack model. *Cryosphere, 8*(1), 257-274. doi:10.5194/tc-8-257-2014

Wever, N., Jonas, T., Fierz, C., & Lehning, M. (2014b). Model simulations of the modulating effect of the snow cover in a rain-on-snow event. *Hydrology and Earth System Sciences, 18*(11), 4657-4669. doi:10.5194/hess-18-4657-2014

Wever, N., Schmid, L., Heilig, A., Eisen, O., Fierz, C., & Lehning, M. (2015). Verification of the multi-layer SNOWPACK model with different water transport schemes. *Cryosphere, 9*(6), 2271-2293. doi:10.5194/tc-9-2271-2015

Wever, N., Würzer, S., Fierz, C., & Lehning, M. (2016). Simulating ice layer formation under the presence of preferential flow in layered snowpacks. *Cryosphere, 10*(6), 2731-2744. doi:10.5194/tc-10-2731-2016

White, A. B., Gottas, D. J., Strem, E. T., Ralph, F. M., & Neiman, P. J. (2002). An Automated Brightband Height Detection Algorithm for Use with Doppler Radar Spectral Moments. *Journal of Atmospheric and Oceanic Technology, 19*(5), 687-697. doi:10.1175/1520-0426(2002)019<0687:AABHDA>2.0.CO;2

Whitfield, P. H., & Pomeroy, J. W. (2016). Changes to flood peaks of a mountain river: implications for analysis of the 2013 flood in the Upper Bow River, Canada. *Hydrol. Process., 30*(25), 4657-4673. doi:10.1002/hyp.10957

Williams, M. W., Erickson, T. A., & Petrzelka, J. L. (2010). Visualizing meltwater flow through snow at the centimetre-to-metre scale using a snow guillotine. *Hydrol. Process., 24*(15), 2098-2110. doi:10.1002/hyp.7630

Würzer, S., Jonas, T., Wever, N., & Lehning, M. (2016). Influence of initial snowpack properties on runoff formation during rain-on-snow events. *J. Hydrometeorol., 17*(6), 1801-1815. doi:10.1175/JHM-D-15-0181.1

Würzer, S., Wever, N., Juras, R., Lehning, M., & Jonas, T. (2017). Modelling liquid water transport in snow under rain-on-snow conditions - considering preferential flow. *Hydrol. Earth Syst. Sci., 21*(3), 1741-1756. doi:10.5194/hess-21-1741-2017

Ye, H., Yang, D., & Robinson, D. (2008). Winter rain on snow and its association with air temperature in northern Eurasia. *Hydrol. Process., 22*(15), 2728-2736. doi:10.1002/hyp.7094

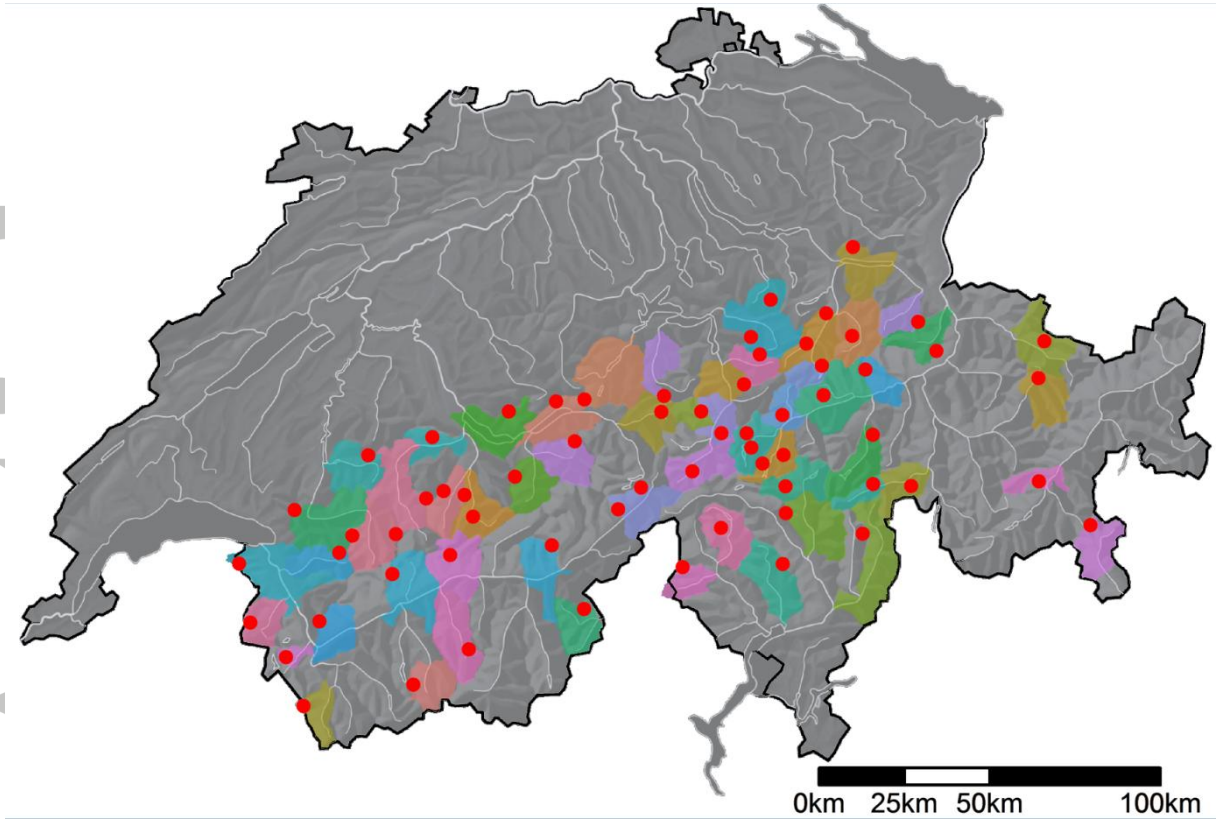

Figure 1: Map of Switzerland with locations of the 58 catchments and 64 IMIS stations used for the analysis.

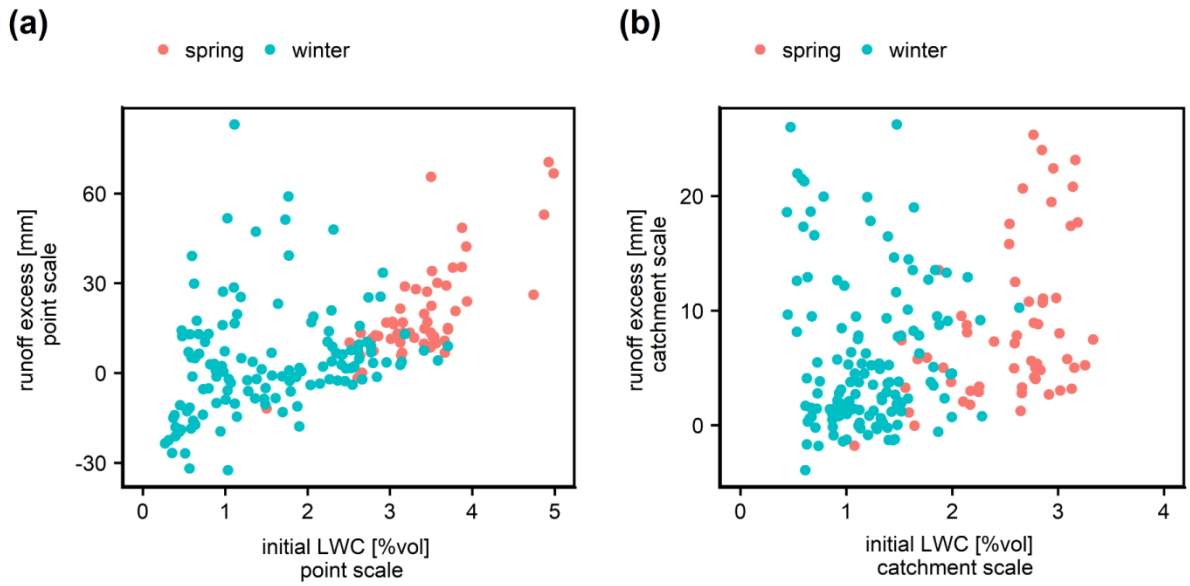

Figure 2: Correlation of runoff excess and snowpack initial liquid water content (LWC) for (a) point and (b) catchment scales. For better visibility, we omitted a point-simulation with initial LWC of 11 %vol and 58 mm runoff excess in (a). The color denotes to spring (April to May) and winter (October to March) events.

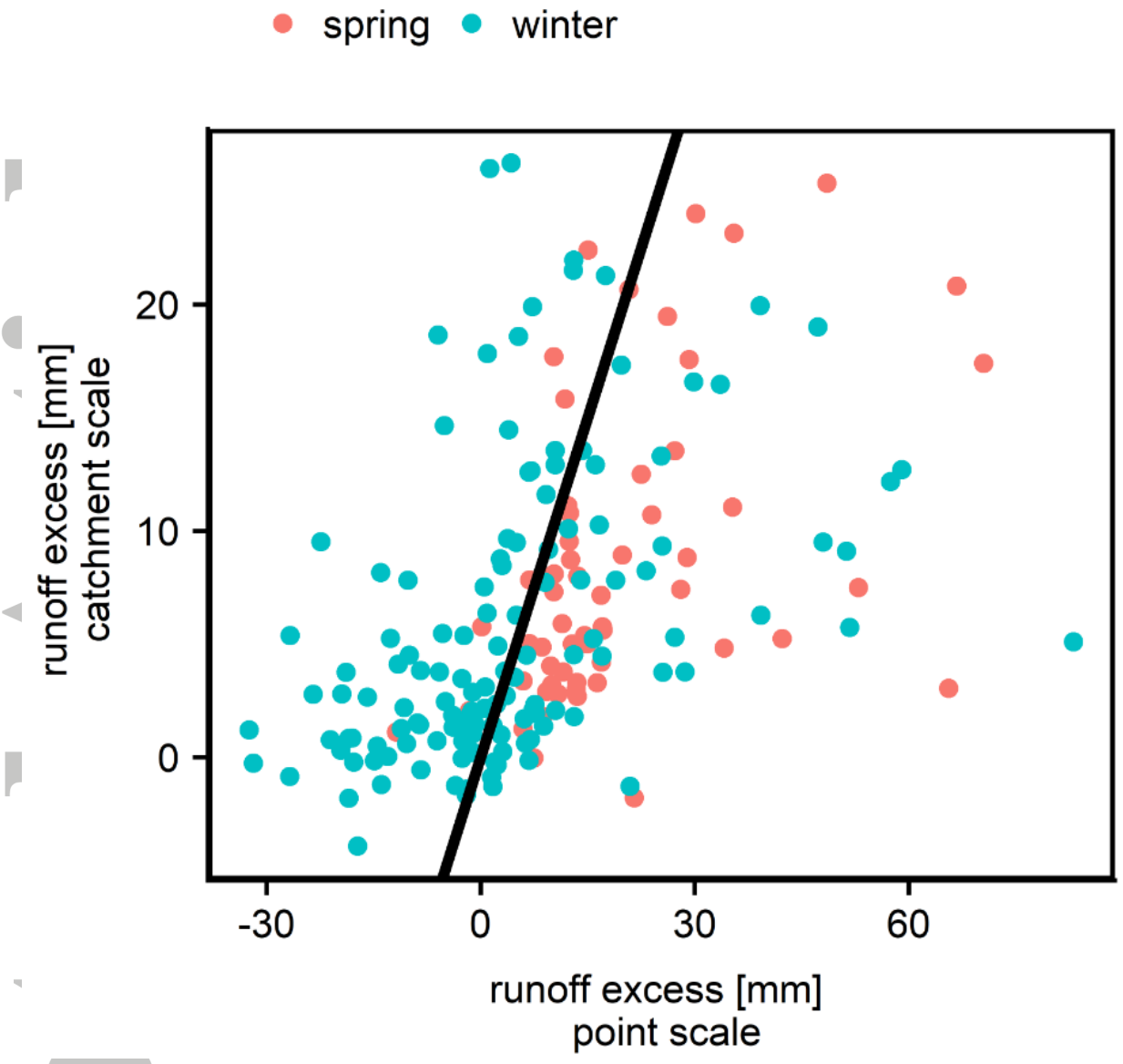

Figure 3: Correlation between runoff excess on the catchment and point scale. The black line denotes to the 1:1 line.

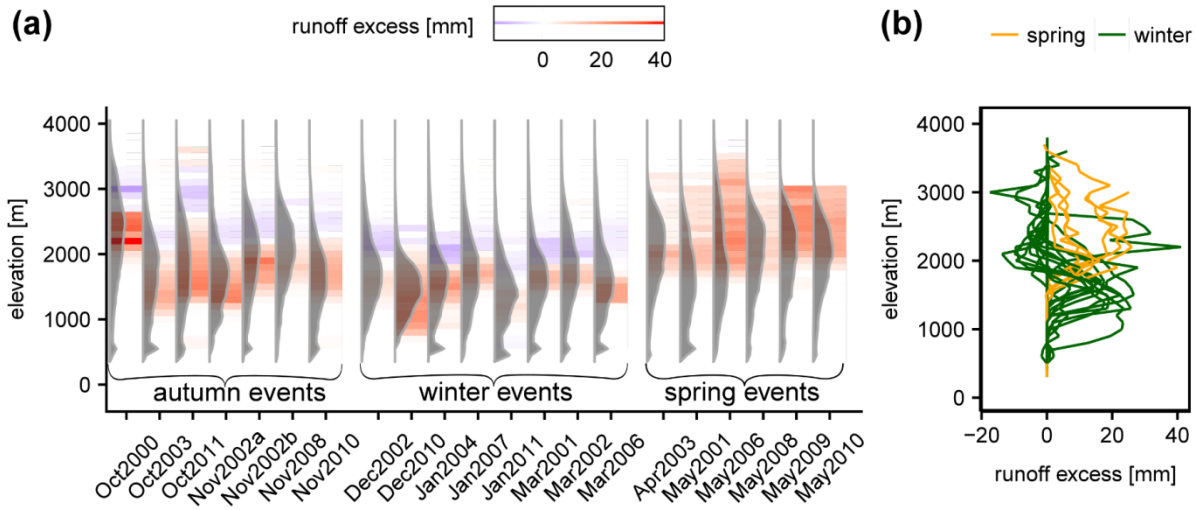

Figure 4: Mean runoff excess as a function of elevation for all 21 events, where results for all CEs associated with the same rain event where evaluated together. The histograms (grey) in (a) display the hypsometry of the affected catchments. Elevational spacing is 100 m. For better visibility, data in (b) is displayed as curves with one point in the center of each 100 m elevation band.

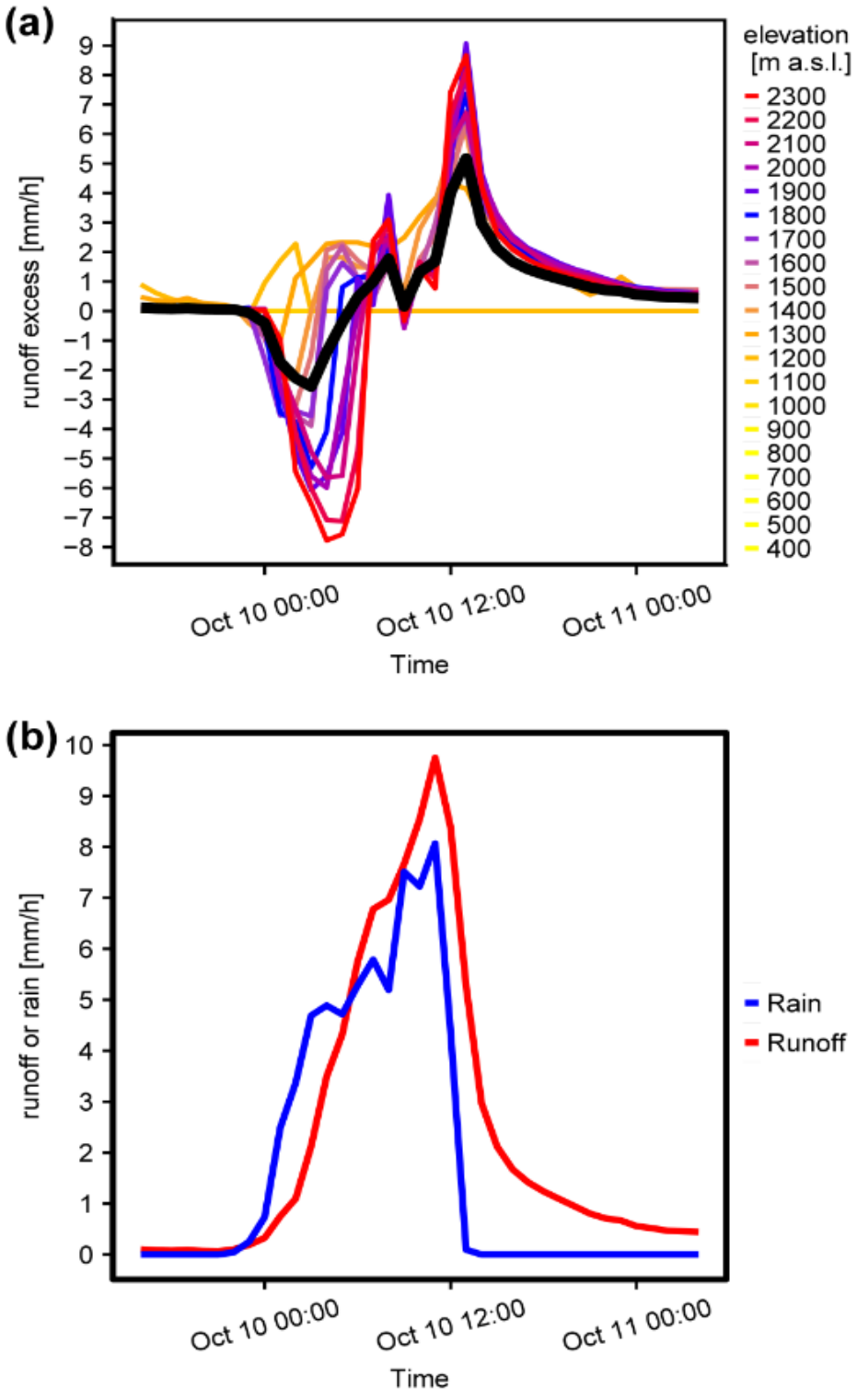

Figure 5: (a) Example of the temporal course of runoff excess in different elevations of a catchment during a ROS event in October 2011. The black line refers to the average. The lowest elevations (< 1100 m) were not covered by snow and therefore overlay each other on the abscissa. Rain and snowpack runoff catchment averages are displayed in (b). We see that runoff excess is negative in the beginning of an event, leading to a delayed increase in runoff. During the course of an event, runoff increase is higher and finally exceeds catchment rain.

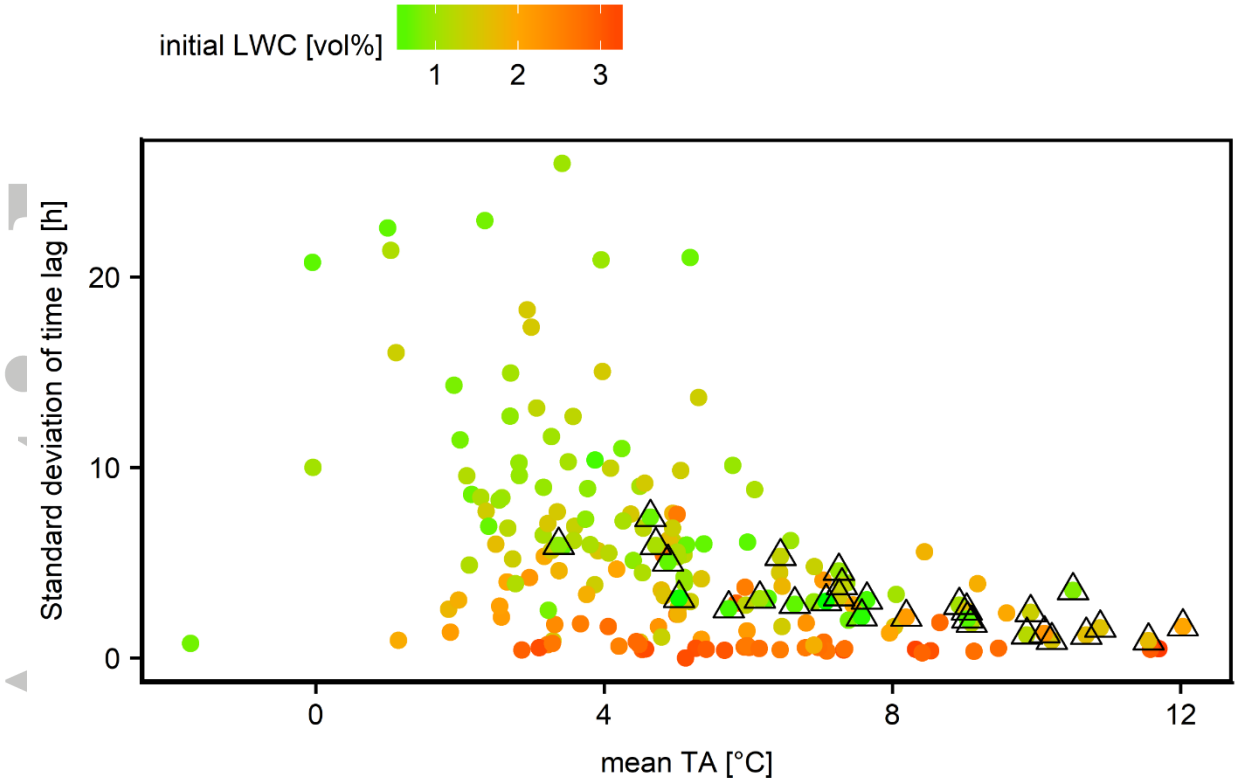

Figure 6: Relationship between standard deviation of the lag time and mean air temperature, where lag time is defined as the time period between onset of rain and onset of runoff. CEs of the October 2011 ROS event are marked with triangles.

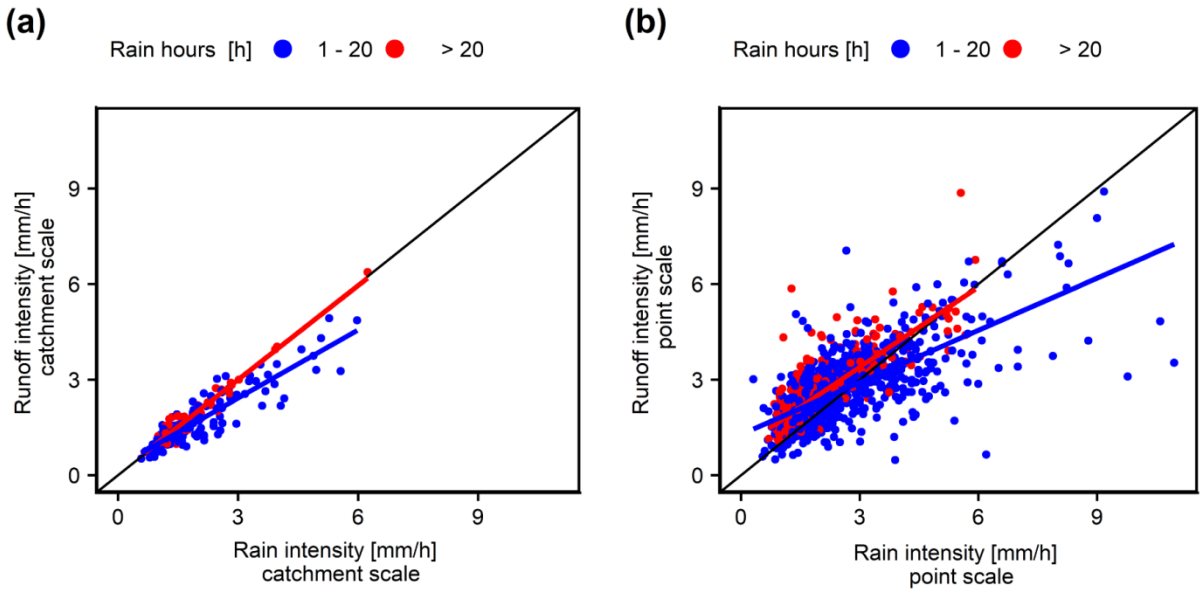

Figure 7: Runoff intensities (averaged over the duration of runoff) vs. rainfall intensities (averaged over the duration of rainfall) for rainfall events of different length for (a) catchment simulations and (b) point simulations of Wuerzer et al. (2016).

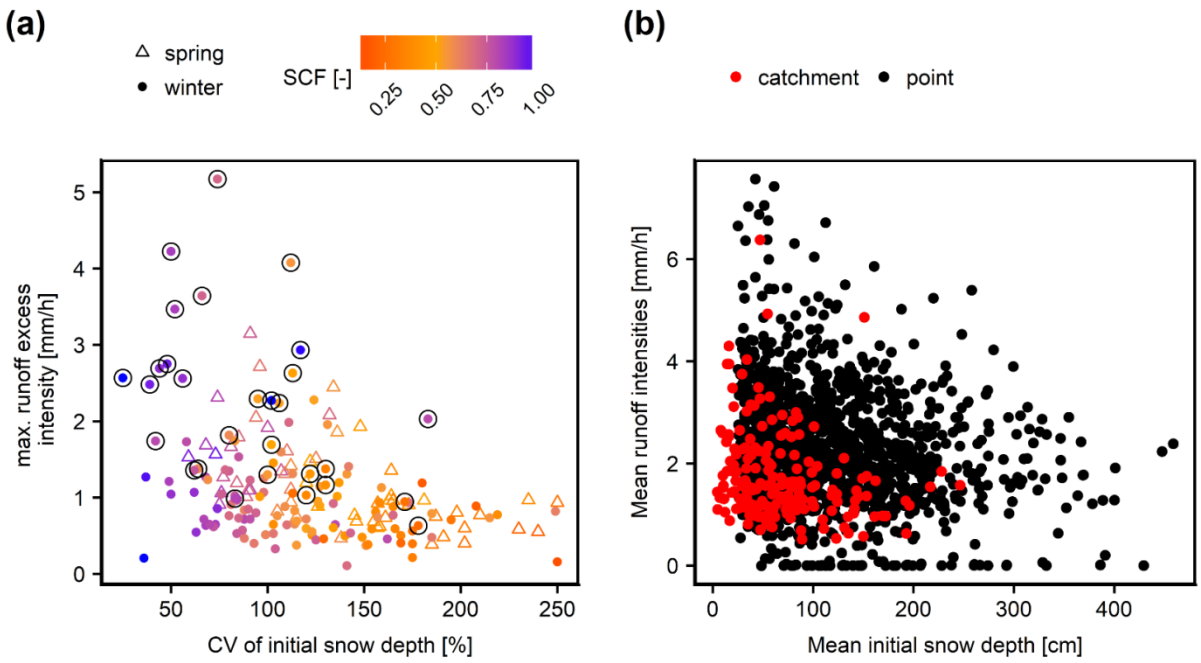

Figure 8: (a) Maximum simulated runoff excess vs. coefficient of variation for initial snow height. Colors show the initial SCF. Circles mark CEs of the October 2011 event. (b) Runoff intensities in terms of the initial snow height for events. Point scale simulations are in black color, the catchment simulations are in red.

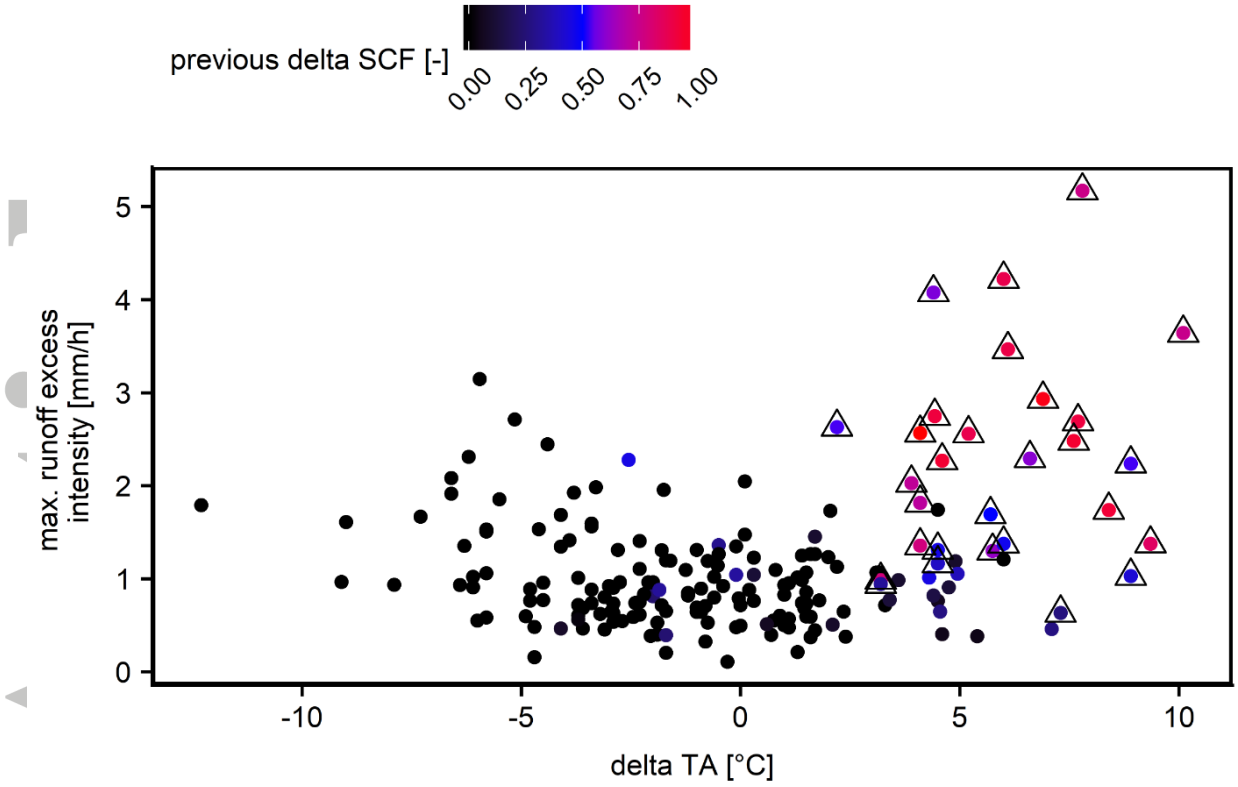

Figure 9: Relationship between maximum runoff excess intensity and the temperature change (delta TA) over the course of the event for all CEs. The color denotes the increase in snow covered fraction (SCF) within the 3 days before the event, i.e. 1 refers to an increase from snow free to fully covered conditions. Triangles mark CEs of the October 2011 event.